POLISH MARITIME RESEARCH Special Issue 2018 S2 (98) 2018 Vol. 25; pp. 23-29
10.2478/pomr-2018-0069

THE INFLUENCE OF SHIP ROLLING MOTION ON TAKE-OFF AERODYNAMIC CHARACTERISTICS OF AIRCRAFT

He Zheng[1], Ph. D.
Sun Xiao-yu[1]*, Ph. D.
Gu Xuan[1]*, Ph. D.
[1]College of Aerospace and Civil Engineering, Harbin Engineering University, Harbin 150001 China

ABSTRACT

Ship motion is an important factor affecting on the safety of ski-jump take-off. The simplified frigate ship SFS1 was numerically simulated, and the results were compared with the experimental data, the feasibility of the calculation method was verified; Meshless method and WALE turbulence model were used to simulate the process of aircraft ski-jump take-off, aerodynamic characteristics under different rolling conditions during the aircraft ski-jump take-off process were presented. The results showed that: the influence of ship rolling motion on lift coefficient, drag coefficient and pitching moment was small, side force and rolling moment were greatly affected by rolling motion; the region of downwash with the maximum speed was about 10 m from the bow; the safety of ski-jump take-off was greatly affected when aircraft was close to the bow within 20 m.

Keywords: Ship rolling motion; Ski-jump take-off; Meshless method; WALE turbulence model; Aerodynamic characteristics

INTRODUCTION

Ski-jump take-off is one of the most important methods of aircraft take-off. Because of the limited ship size, the six degree of freedom motion of the ship and the upwash flow near the bow, taking off on ship is more complex than taking off on land, the security of ski-jump take-off has attracted increasing attention [1, 2]. While researching, not only the aerodynamic characteristics of the aircraft at different wind directions, wind speeds, the speed of departure and the angle of attack should be considered, the effects of ship rolling, pitching and heaving are also considered [3]. Hong W. H. established various forms of superstructure and changed the vertical layout of the superstructure, numerical simulations were respectively carried out, the flow field is analyzed and observed, and the characteristics of the flow field were compared [4]. Wang W. J. aimed at the characteristics of the aircraft taking off on the skid deck, the fitting relationship between the performance and quality of the aircraft and deck parameters was analyzed based on the changing process of the force polygon and the effect of the deck shape on the pitching rotation, the mechanical mechanism of the aircraft establishing the angle of attack in the early departure at low speed was presented [5]. Liu W. W. established a general mathematical model of aircraft take-off based on tensor [6]. Wang M. H. and Zhao B. described the different methods of aircraft take-off and landing process, some key factors in the take-off and landing process are presented [7]. The take-off speed and the landing speed were estimated and analyzed based on the characteristics of the aircraft by Chen B. and Ang H. S. [8]. Gregory Imhof and William Schork discussed the influence of the skid deck curve on the take-off of the aircraft, and the optimization is carried out [9]. P. Shrikant Rao and Amitabh Saraf proposed a method for analyzing the performance of ski-jump take-off, some flight parameters were optimized and a set of feedback control system is designed [10]. The distribution of airflow around the warship was studied by Gao Y. and Xie H. S. [11]. The difference of the airflow distribution in different conditions was obtained, the influence during the course of the aircraft ramp ski-jump take-off on the airflow distribution on the deck was also considered. The result showed that the airflow distribution around the warship was considerably complicated and the influence on the air dynamic characteristics for the aircraft take-off can't be

neglected [12]. The sideslip wind would greatly enhance the airflow's turbulent intensity on the deck. Bi Y. Q. and Sun W. S. established a mathematical model of aircraft take-off and carried out a numerical simulation for a certain fighter aircraft [13]. The effect of take-off mass, take-off angle of attack, deck wind, take-off distance and other factors on the performance of the ski-jump take-off was quantitatively analyzed. Xiao H. introduced the principle and motility characteristics of the ski jump take-off, the mathematical model of ski jump take-off was given [14]. Take-off performance of aircraft under different configurations was simulated, the influence of take-off distance, take-off weight and fight trim on the ski jump take-off performance was analyzed. Gao Y. used dynamic mesh technology and the Spalart-Allmaras turbulence model to simulate aircraft ski-jump take-off from a ramp deck [15]. Aerodynamic characteristics during the aircraft ski-jump take-off process were analyzed under many different conditions. The result shows that improvements in the take-off aerodynamic characteristics for aircraft require taking off at an optimal airspeed. Bai S. G. established the six degrees of freedom model of aircraft in the condition of static balance, with the influences of carrier movement, deck wind and the airflow interference on aircraft considered [16, 17]. The static balance of aircraft in different situations was simulated, and the motion law of aircraft under different conditions was analyzed.

Overall, the research of aircraft ski-jump take-off is mainly focused on the following aspects: ramp deck curvature optimization, take-off decision, the analysis of aircraft motion characteristics, the influence of superstructure layout on airflow field and so on [18]. The research on the influence of ship rolling on the aircraft take-off is relatively less.

In recent years, many international scholars propose and develop the mesoscopic theories combining the macroscopic fluid mechanics with the microscopic molecular dynamics. Mesoscopic numerical models based on the Boltzmann equation of molecular motion theory are developed to reproduce the gas flow problem with a characteristic scale of micron and nanometer, Lattice Boltzmann method (LBM) is one of them [19, 20]. Compared with the traditional computational fluid dynamics method, this method can deal with more complicated boundary conditions and there is no need to mesh in the fluid domain. It has a great advantage in the CFD calculation of complex geometry. In this paper, the influence of ship rolling motion on the aerodynamic characteristics of aircraft during take-off is studied.

CALCULATION METHOD

LATTICE BOLTZMANN METHOD (LBM)

The Lattice Boltzmann Method (LBM) makes use of statistical distribution functions with real variables, preserving by construction the conservation of mass, linear momentum and energy. The collision operator is simplified under the Bhatnagar-Gross-Krook (BGK) approximation, it's defined as follows:

$$\Omega_i^{BGK} = \frac{1}{\tau}\left(f_i^{eq} - f_i\right) \tag{1}$$

Where τ is the relaxation characteristic time (which is related to the macroscopic viscosity) and f_i^{eq} is the local equilibrium function.

The equilibrium distribution function usually adopts the following expression:

$$f_i^{eq}(\gamma,t) = t_i\rho\left[1+\frac{c_{i\alpha}v_\alpha}{c_s^2}+\frac{v_\alpha v_\beta}{2c_s^2}\left(\frac{c_{i\alpha}c_{i\beta}}{c_s^2}-\delta_{\alpha\beta}\right)\right] \tag{2}$$

Where c_s is the sound speed, v is the macroscopic velocity, δ is the Kronecker delta, and ti are built preserving the isotropy in space.

WALE TURBULENCE MODEL

WALE model is chosen to be turbulence model This model recovers the asymptotic behavior of the turbulent boundary layer when this layer can be directly solved and it does not add artificial turbulent viscosity in the shear regions out of the wake. The WALE model is formulated as follows:

$$v_{\text{turbulent}} = \Delta^2\frac{\left(G_{\alpha\beta}^d G_{\alpha\beta}^d\right)^{3/2}}{\left(S_{\alpha\beta}S_{\alpha\beta}\right)^{5/2}+\left(G_{\alpha\beta}^d G_{\alpha\beta}^d\right)^{5/4}} \tag{3}$$

$$S_{\alpha\beta} = \frac{1}{2}\left(\frac{\partial v_\alpha}{\partial r_\beta}+\frac{\partial v_\beta}{\partial r_\alpha}\right) \tag{4}$$

$$G_{\alpha\beta}^d = \frac{1}{2}\left(g_{\alpha\beta}^2+g_{\beta\alpha}^2\right)-\frac{1}{3}\delta_{\alpha\beta}g_{\gamma\gamma}^2 \tag{5}$$

$$g_{\alpha\beta} = \frac{\partial v_\alpha}{\partial r_\beta} \tag{6}$$

$$\Delta = C_w \text{Vol}^{1/3} \tag{7}$$

Where Δ is the filter scale, S is the strain rate tensor of the resolved scale, and C_w (the WALE constant) is typically 0.2.

VERIFICATION CALCULATION

PHYSICAL MODEL

Simplified frigate ship SFS1 is the simulation model of Verification Calculation. The model measures about 138.7 m long × 13.7 m wide × 16.8 m deep, its specific dimensions refer to the reference documentation. Simplified frigate ship SFS1 is shown in Fig. 1.

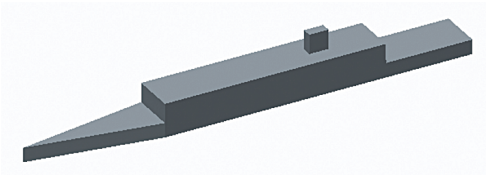

Fig. 1. SFS1 model

CALCULATION CONDITIONS AND SETTINGS

The computational domain uses the virtual wind tunnel in the simulation of simplified frigate ship SFS1. The ship model remains stationary and the wind direction is windward. The inlet wind speed is 20 m/s, the surface of the ship is no-slip wall, and the sea level is set as frictionless wall.

CALCULATION RESULTS AND ANALYSIS

A horizontal line is chosen in the computational domain. It's on the vertical plane in the middle of the flight deck, and the line is same height as the top of the hangar.

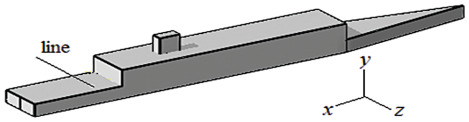

Fig. 2. Schematic diagram of monitoring line

The simulation results are compared with the literature, as shown in Fig. 3. The X axis is the ratio of the Z direction coordinate to the flight deck width, and the Y axis is the dimensionless ratio of the velocity component.

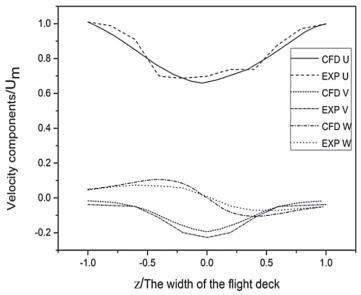

Fig. 3. Dimensionless velocity components in the middle of flight deck

From the Fig. 3., the simulation results are in good agreement with the experimental data, the calculation method is verified. The result of Z directional velocity component shows that the directions of velocity on both sides are opposite, airflow flows from side to the middle, and the velocity magnitude is symmetrical. The result of Y directional velocity component shows that there is dowmwash above the flight deck.

SIMULATIONS IN DIFFERENT SHIP ROLLING CONDITIONS

PHYSICAL MODEL

Simulation model is shown in Fig.4:

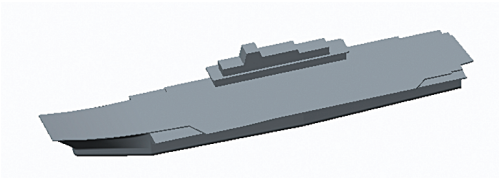

(a) aircraft carrier model

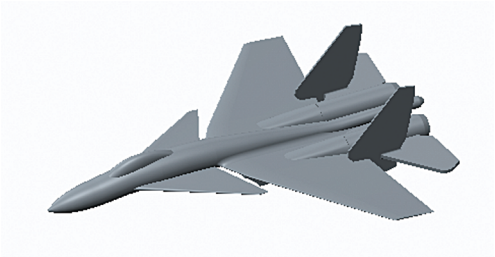

(b) aircraft model

Fig. 4. Simulation model

CALCULATION CONDITIONS AND SETTINGS

The computational domain uses the virtual wind tunnel in the simulation of aircraft take-off. The ship model remains stationary and the wind direction is windward. The inlet wind speed is 25 m/s, and the initial velocity of aircraft is 0 m/s. Aircraft moves and leaves the deck with 40 m/s2 acceleration, the total movement time is 2.4 s. In this process, the rolling motion of the aircraft carrier accords with the sine function, the swing amplitude is 3° (the angle toward to starboard is positive, otherwise it's negative), and the rolling period is 8 s. The surface of ship and aircraft is no-slip wall, and the sea level is set as frictionless wall. There is a refinement region around aircraft and the bow, as shown in Fig. 5.

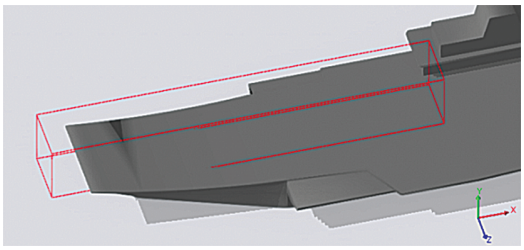

Fig. 5. Schematic diagram of refinement region

In order to analyze conveniently, the landing process of aircraft is divided into two sections: horizontal deck section (0 s–1.5 s) and skid deck section (1.5 s–2.4 s).

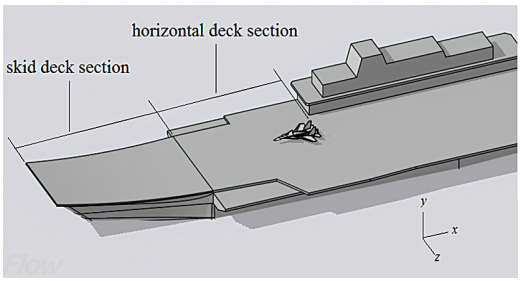

Fig. 6. Schematic diagram of aircraft

CALCULATION RESULTS AND ANALYSIS

Because the aircraft take-off time is smaller than ship rolling period, different rolling conditions should be considered. There are 8 calculation conditions in this paper. In order to facilitate the analysis, the calculation condition which ship remains stationary is represented as JZ, the rest of them are shown in Tab. 1.

Tab. 1. Ship rolling calculation conditions

Calculation conditions		Initial rolling angle				
		-3°	-1.5°	0°	1.5°	3°
Rolling direction	Starboard (R)	R-3	R-1.5	R0	R1.5	—
	Port (L)	—	L-1.5	L0	L1.5	L3

When the initial angle of the hull is 0° and deflects to the starboard, the vortices of the carrier takeoff process are shown in Fig. 7.

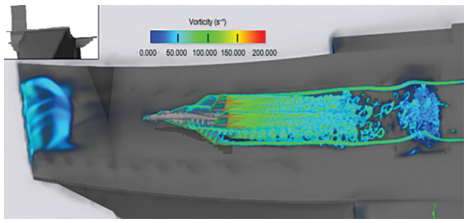

Fig. 7. Vorticity contours in 2 s

It can be seen from Fig. 7. that the larger vorticity region is mainly present on the carrier's tail and the route of its movement. In addition, there is a significant vortex structure in the bow part, which is caused by the flow around the ship, and the aerodynamic characteristics and force of the aircraft will change when the carrier is slipping off the area near the bow. Since the calculation is only encrypted around the flight path, the vortices on both sides of the bow are less noticeable than the encrypted area.

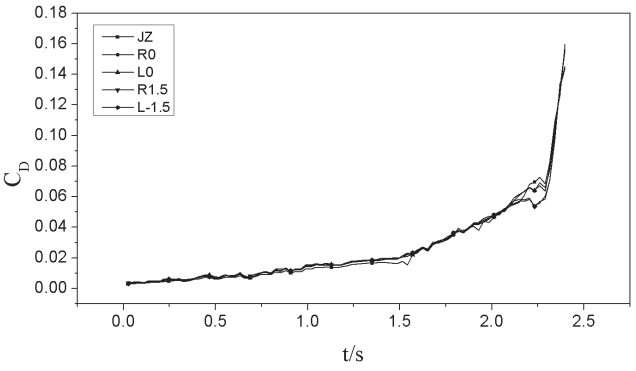

(a)

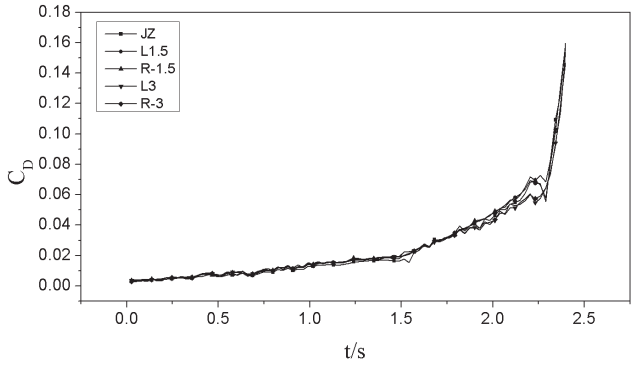

(b)

Fig. 8. The drag coefficient

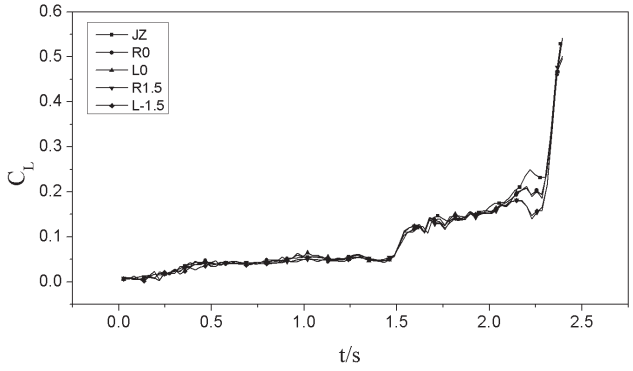

(a)

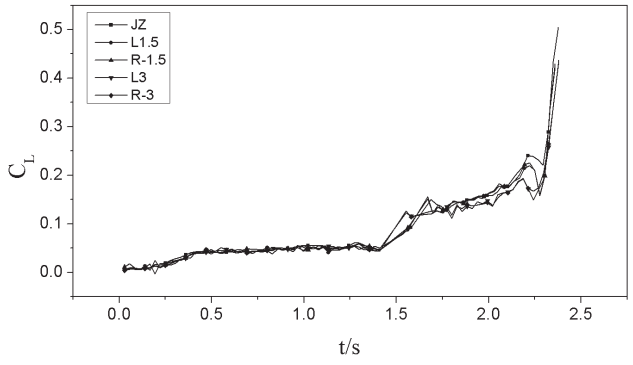

(b)

Fig. 9. The lift coefficient

Fig. 8. and Fig. 9. show the drag coefficient and lift coefficient of carrier-based aircraft under different roll conditions. Compared with the calculated results, it can be found that the variation of the drag coefficient and the lift coefficient are basically the same under different working conditions. In the horizontal deck section (0–1.5 s), because the aircraft angle of attack is zero, the resistance coefficient and the lift coefficient are increasing with the speed increases slowly;In the skid deck section (1.5–2.4 s), the speed of the aircraft is increasing, and the angle of attack is also increasing, relative to the horizontal deck section, the resistance coefficient and the lift coefficient rise faster. In addition, it can be seen from the curve of the lift coefficient of the skid deck section, which shows that the growth rate of the front lift coefficient is much smaller than that of the rear, which shows that the aerodynamic characteristics of the aircraft in the front of the skid deck are relatively poor.

On the skid deck, the six horizontal monitoring lines shown in Figure 10 are 20 m in length (z = –10 m to z = 10 m), and the height of the skate deck surface is 2 m, line 1–6 Z = 13.1 m, profile x = –142 m, y = 13.9 m, profile x = –148 m, y = 14.8 m, section x = –146 m, y = 12.4 m, X = –154 m, y = 15.8 m, profile x = –160 m, y = 16.9 m.

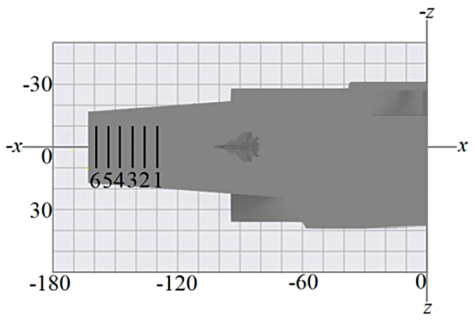

Fig. 10. Schematic diagram of monitoring line

The velocity component (ie velocity component v) of the six monitoring lines on the monitoring line at t = 1.7 s is shown in Fig. 11. when the hull does not roll motion.

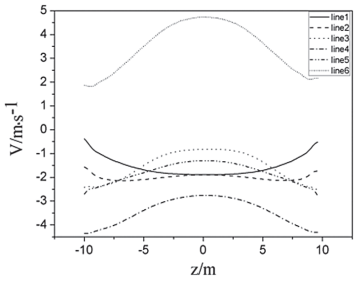

Fig. 11. Velocity components of Y direction in different monitoring line

It can be seen from the figure, 1–5 line at the existence of the next wash gas flow, and the next washing air flow rate is fastestin the 5th line, and there is the 6th line on the wash stream. When the aircraft slides throught line 1–5, it is affected by the underwent airflow. When it continues to travel to line 6, it will be affected by the upper airflow. The lift factor of the skid deck will show as shown in Fig. 9.

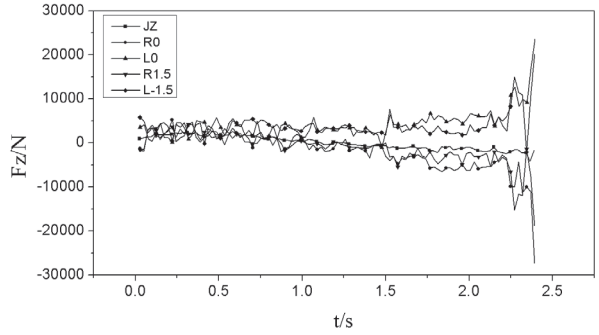

(a)

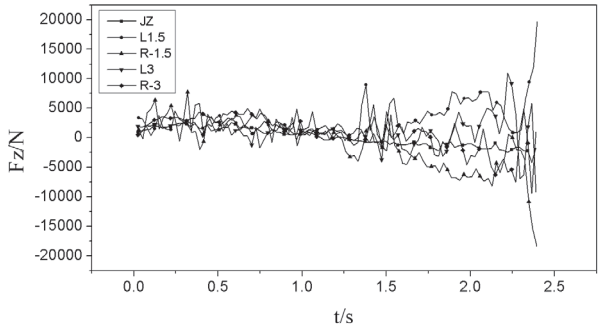

(b)

Fig. 12. Side force of aircraft

It can be seen from the figure, the aircraft carrier does not occur when the roll, due to the wind direction for the wind, the aircraft by the lateral force relative to the roll movement is very small, and little change; when the aircraft carrier roll. The lateral force in the horizontal deck section is relatively small and the lateral force in the skid deck section is greater, especially in the period of t = 2.2 s to t = 2.4 s, which is due to the fact that the aircraft is traveling. To the skid deck section, due to their own deflection angle and the impact of the bow airflow disturbance, in the skid deck section of the greater the angle of the aircraft carrier, the greater the lateral force of the aircraft. In addition, the aircraft carrier roll movement, the aircraft in the skid deck section by the direction of lateral force and roll deflection direction is basically the same, that is, when the aircraft carrier to the deck on the right side, the body force is also biased to the right, and vice versa also else.

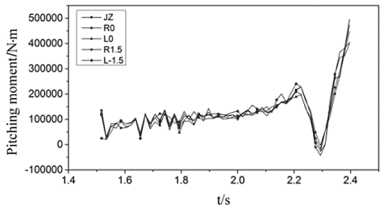

(a)

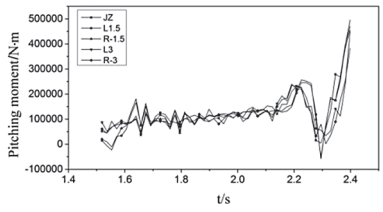

(b)

Fig. 13. Pitching moment of aircraft (Skid deck section)

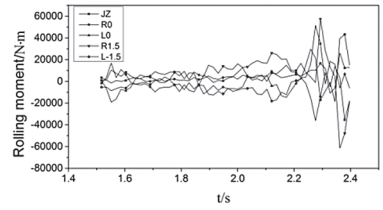

(a)

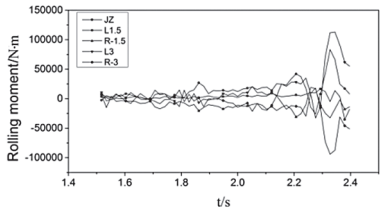

(b)

Fig. 14. Rolling moment of aircraft (Skid deck section)

As can be seen from Fig. 13. and Fig. 14., the roll motion of the aircraft carrier has little effect on the pitch torque of the aircraft in the skid deck section and has a greater effect on the roll torque, especially at t = 2.2 s to t = 2.4 S during the period of time, the aircraft through the x = -144 m to x = -164 m deck area.

CONCLUSION

The impact of the carrier roll on the lift coefficient, drag coefficient and pitching torque of the aircraft during the takeoff of the carrier is small, which has a great influence on the lateral force and the rolling moment.

When the aircraft enters the skid deck section, it is affected by the underwent airflow, which is affected by the upper airflow near the bow, resulting in a relatively small lift coefficient of the aircraft in the front of the skid deck. The aerodynamic characteristics are relatively The area where the maximum velocity of the lower wash airflow is located is about 10 m from the bow.

(3) In the case of a roll, the lateral force of the aircraft in the horizontal deck section is much smaller than that of the skid deck. The greater the deflection angle in the skid deck section, the greater the lateral force of the aircraft. In addition, when the aircraft carrier is rolling, the lateral force and the rolling moment of the aircraft are large and change rapidly in the area of about 20 m from the bow to the end of the skid deck. The area is the most affected by the flight.

ACKNOWLEDGEMENTS

This work is supported financially by the National Natural Science Foundation of China(No. 11602066).

REFERENCES

1. W. H. Hong, Z. F. Jiang, T. Wang.: *Influence of Upper Building Form and Layout on Ship 's Air Flow Field*, Chinese Ship R., Vol. 2, no. 2, pp. 53–68, 2009.
2. W. J. Wang, L. L. Guo, X. J. Qu.: *Analysis of Mechanics Mechanism of Skidding*, Beijing University.Aero. Astron.J., Vol. 34, no. 8, pp. 887–889, 2008.
3. W. W. Liu, X. J. Qu.: *Kinetic Modeling of Slip – like Takeoff Based on Tension* , Chinese Aero,J., Vol. 18, no. 4, pp. 326–335, 2005.
4. M .H. Wang, B. Zhao.: *Study on the Dynamics of Shipborne Aircraft*, Chinese Aircraft Design.J., Vol. 2, no. 1, pp. 23–33, 1997.
5. B. Chen, H. S. Ang.: *Characteristics and Performance Analysis of Shipborne Aircraft*, Chinese Jiangsu Airlines. J., Vol. 3, no. 3, pp. 2–5, 2011.
6. I. Gregory, S. William.: *Using simulation to optimize ski jump ramp profiles for STOVLE aircraft*, AIAA-2000-4285, Vol. 2, no. 2, pp. 53–58, 2000.
7. R. P. Shrikant, S. Amitabh.: *Performance analysis and control design for ski-jump take off*, AIAA-2003-5412, Vol. 4, no. 2, pp. 43–48, 2003.
8. Y. Gao, H. S. Xie.: *Numerical Simulation of Flow Field around Hull in Slip – off Process*, Chinese Aero.J., Vol. 26, no. 4, pp. 513–518, 2008.
9. Y. Q. Bi, W. S. Sun.: *Preliminary Analysis on Take – off Performance of a CertainType of Fighters*, Flight mech.J., Vol. 26, no. 4, pp. 18–21, 2006.
10. H. Xiao, S. M. Yang, J. Y. Yu.: *Simulation Analysis of Takeoff Performance of a Certain Type of Aircraft*, Flight mech. J., Vol. 27, no. 4, pp. 78–80, 2009.
11. Y. Gao, X. Gu, H. S. Xie, Z. He.: *Optimum Selection and Pneumatic Characteristicsof Take – off Parameters of Shipboard Sliding*, Harbin Engineer University.J., Vol. 29, no. 10, pp. 1040–1045, 2008.
12. S. G. Bai, M. Q. Hu, J. T. Dun.: *Six – degree – of – freedom static balance analysis of carrier – borne ejection*, Air Force Engineer University.J., Vol. 13, no. 3, pp. 21–24, 2012.
13. D. Tian.: *The Principle and Application of Lattice Boltzmann Method*, Daqing: Daqing Petrol.Instit., China, 2009.
14. Y. H. Qian, D. D'humieres, P. Lallemand.: *Lattice BGK models for Navier-Stokes equation*, Europhysics L., Vol. 17, no. 6, pp. 479–484, 1992.
15. S. Y. Chen, G. Doolen.: *Lattice Bolzmann method for fluid flows*, Fluid Mech Annual.R., Vol. 30, no. 2, pp. 329–364, 1998.
16. S. Succi.: *The Lattice Boltzmann Equation for Fluid Dynamics and Beyond*. Clarendon Press,United Kingdom,2001.
17. M. Liu, X. P. Chen, N. Kannan. Premnath.: *Comparative Study of the Large Eddy Simulations with the Lattice Boltzmann Method Using the Wall-Adapting Local Eddy-Viscosity and Vreman Subgrid Scale Models*, Chinese Phys.L., Vol. 29, no. 10, pp. 104706–104710, 2012.
18. D. M. Roper, I. Owen, G. D. Padfield, S. J. Hodge.: *Integrating CFD and piloted simulation to quantify ship–helicopter operating limits*, Aero.J., Vol. 110, no. 119, pp. 419–428, 2006.
19. James Forrest, I. Owen.: *An investigation of ship airwakes using Detached-Eddy Simulation*, Comp.Fluid.J, Vol. 39, no. 4, pp. 656–673, 2010.
20. S. M. Zhou.: *Simulation Analysis on the Influence of Carrier Deck Movementon Shipboard Carrier*, Aircraft design.J., Vol. 32, no. 6, pp. 28–32, 2012.

CONTACT WITH THE AUTHOR

Sun Xiao-yu, Ph.D.
e-mail: sunxiaoyu520634@163.com
tel: 13258668951
College of Aerospace and Civil Engineering Harbin
Engineering University
Harbin 150001
China